Exciton complexes in $In_xGa_{1-x}As/GaAs$ quantum dots

M. Bayer, T. Gutbrod, and A. Forchel
Technische Physik, Universität Würzburg, Am Hubland, D-97074 Würzburg, Germany

V. D. Kulakovskii and A. Gorbunov
Institute of Solid State Physics, Russian Academy of Sciences, 142432 Chernogolovka, Russia

M. Michel, R. Steffen, and K. H. Wang
Technische Physik, Universität Würzburg, Am Hubland, D-97074 Würzburg, Germany

(Received 1 August 1997; revised manuscript received 17 March 1998)

Multiexciton complexes in $In_xGa_{1-x}As/GaAs$ quantum dots in the weak-confinement regime have been investigated by photoluminescence spectroscopy at $T=2$K. The lateral dot sizes varied down to about 50 nm so that the transition from the quantum well to the quantum dot case could be studied. The biexciton binding energy $\Delta(X_2)$ increases with decreasing dot size, depending on the height of the confinement potential. The splitting of the biexciton emission by a magnetic field ($B \leqslant 8$ T) arises from the spin splitting of the exciton in the final state of the optical transition, because the biexciton is a spin-singlet state. A magnetic field reduces $\Delta(X_2)$ by approximately the exciton spin splitting. This reduction is due to the decrease of the energy gap between the biexciton transition into the spin ground-state of the exciton and the transition of the spin ground-state exciton. The formation of complexes consisting of three and four excitons becomes possible due to the three-dimensional quantum dot confinement. Because of the Pauli principle the Coulomb correlations in the three-exciton complex result in a net repulsion energy that increases strongly with decreasing dot size. The multiexciton interaction energies are reduced by a magnetic field because the exciton repulsion decreases when the magnetic length becomes smaller than the quantum dot size. In the four-exciton-complex we find an exchange energy splitting of states corresponding to carrier configurations with parallel and antiparallel spins. The energy differences between exciton transitions from excited and ground states are about equal to the corresponding energy splittings of the single-particle electron and hole states. These findings indicate that the strong Pauli repulsion between electrons and holes determines the formation of exciton complexes. Based on these results a shell model for quantum dot multiexciton states is discussed. [S0163-1829(98)05232-1]

I. INTRODUCTION

Optical studies of semiconductor quantum dots (QD's) might open new possibilities for investigating Coulomb interactions in multiparticle states consisting of electrons (e's)/holes (h's), or excitons (X's). This expectation is supported by the development of several fabrication techniques capable of providing high-quality QD's.[1] For example, QD's have been formed by embedding semiconductor microcrystals in glass matrices. Other techniques make use of epitaxial growth, by which QD's can be fabricated either directly, e.g., by self-organized growth, or by means of lithographic patterning of quantum wells (QW's).

The confined nature of the single-particle states in QD's has been shown by various techniques of optical spectroscopy.[1] Multiparticle effects are of importance in a variety of aspects of the linear and nonlinear optical properties of semiconductor quantum structures.[2] The formation of multiparticle complexes in QD's is determined by the discrete, atomiclike level structure and by the strong Coulomb interactions among the carriers. The interplay of these effects might cause new collective phenomena. A particular example are the ''magic'' states in doped QD's: the total angular momentum of a certain number of e's is driven through a sequence of discrete values by a magnetic field because of the competition between kinetic energy and e-e repulsion.[3,4]

The goal of this paper is to study QD multiparticle states consisting of several X's. A well-known example of such a complex is the biexciton (biX) consisting of two X's. In bulk crystals the biX is bound only by the Coulomb interaction between the carriers. Only the spin-singlet biX state is stable, while the triplet state is unstable due to the strong Pauli-repulsion between carriers with identical spin orientations.[5] The effect of quantum confinement on the biX has been studied widely in QW's and a strong enhancement of the biX binding energy over the bulk value has been found.[5,6] In quantum wires no experimental observation of biX formation has been reported up to now, although calculations predict a drastic increase of the binding energy.[7,8]

BiX's in QD's have been subject of a number of theoretical investigations of the influences of geometric and dielectric confinement on their binding energies.[9–16] Experimentally, biX's in microcrystals[9] have been studied by linear and nonlinear spectroscopy. A systematic increase of the ground-state biX binding energy with decreasing dot size has been found, in good agreement with model calculations.[14,17] Also, excited biX states have been observed and even lasing involving biX's was found.[14,17] In III-V semiconductors the biX binding energy is clearly smaller than in wide-gap semiconductors. Therefore single-dot spectroscopy has been applied to observe biX's.[18,19] Also, here an increase of the biX binding energy was observed, e.g., for $GaAs/Al_xGa_{1-x}As$

QD's with sizes comparable to the X Bohr radius a_x by more than one order of magnitude over the bulk value.[18]

Similar to the biX triplet state, multiexcitons (multiX's) consisting of more than two excitons are not stable in semiconductors with simple conduction and valence-band structures because of the Pauli repulsion. However, in QD's the geometric confinement prevents a separation of X's in space and thus enables the formation of multiX's.

In photoluminescence studies using high optical excitation QD's have been occupied with more than two electron-hole pairs. The spectral features in the emission of QD multiX's are still not fully understood. For example, a Fermi gas of excitons has been proposed from time-resolved experiments on single QD's.[20] In studies on QD arrays the formation of an electron-hole plasma has been suggested.[21–25] However, in these experiments surprisingly no ''band-gap renormalization'' was observed. Recently, the first clear observation of a three-exciton complex in QD's has been claimed for CuCl microcrystals embedded in a NaCl matrix.[26]

Only a few theoretical studies exist up to now on multiexciton complexes.[27,28] For self-organized QD's with sizes comparable to the X Bohr radius it was shown that the strongly correlated e's and h's in a QD form a gas of weakly interacting X's.[28] The origin for this behavior lies in hidden symmetries of the multiparticle Hamiltonian, which are based on degeneracies of QD states from geometrical invariances and on the symmetry of the interparticle Coulomb interactions. Because of these symmetries the chemical potential shows pronounced plateaus as function of the X density in the dot reflecting the single-particle density of states. Both addition and subtraction of an X in a shell occurs only within a small set of allowed energies and leads to a fine structure of the emission spectrum. In lowest approximation the splitting among the emission features from different X complex shells is given by the energy splitting of the single-particle states. However, the Coulomb interaction causes a renormalization of the transition energies of the exciton droplet and the oscillator strengths.

In the present paper we investigate the X-X interactions in X complexes in QD's in the weak-confinement regime, where the dot size is larger than the X Bohr radius. When done on QD arrays, such studies are often complicated by the inhomogeneous broadening of the emission due to dot size fluctuations. These broadening effects in the optical spectra prevent a resolution of the fine structure due to X-X interaction. Therefore the present experiments were performed on $In_{0.14}Ga_{0.86}As/GaAs$ single QD's and on arrays of $In_{0.03}Ga_{0.97}As/GaAs$ QD's, whose spectra show only a small broadening.

First we study the dependence of the biX binding energy $\Delta(X_2)$ on dot size and on confinement potential height. For large confinement potentials we find a strong increase with decreasing dot radius, while for weakly confined QD's the binding energy is almost independent of dot size. We also study the dependence of $\Delta(X_2)$ on magnetic field. In addition, we investigate the interaction energies in multiX's consisting of more than two X's. The correlation energies increase strongly with decreasing dot size and they are strongly reduced when applying a magnetic field. For the four-exciton complex we find an energy splitting, which can be related to the exchange energy splitting of carrier configurations with parallel and antiparallel spins.

The outline of the paper is as follows: In Sec. II we give a description of the QD samples and of the experimental technique used to study these structures. The results of the investigation of biX's are given in Secs. III and IV we present the results for multiX complexes consisting of several X's.

II. EXPERIMENTAL

The experiments were performed on undoped QD's fabricated by lithography and etching on $In_xGa_{1-x}As/GaAs$ QW's.[29] The samples were held at a temperature of 1.5 K in the Helium insert of an optical magnetocryostat ($B \leqslant 8$ T) with the field aligned normal to the heterostructure. For optical excitation we used an Ar^+ laser. The laser spot could be focused down to a diameter of about 20 μm with a variable excitation power up to 1 kW cm^{-2}. In order to avoid sample heating effects, the average laser power incident on the sample was limited to 50 W cm^{-2} by a mechanical chopper when using high excitation. The emission was dispersed by a monochromator ($f=0.6$ m) and detected by a LN_2-cooled Si charge-coupled-devices camera. The polarization of the luminescence could be analyzed by a quarter-wave retarder and linear polarizers.

To study the rather small confinement-induced changes of the Coulomb interaction between carriers in a QD, effects of sample inhomogeneities must be avoided or at least decreased. Such inhomogeneities cause a strong broadening of optical spectra hiding thus Coulomb interaction effects. In the present experiments they were suppressed by properly designed samples:

(i) First we have studied single QD's of cylindrical and rectangular shape. Starting material was an $In_{0.14}Ga_{0.86}As/GaAs$ QW with a width of 5 nm. From this QW single QD's of widely varying sizes were fabricated. The spacing between adjacent dots was 50 μm, so that the laser spot (with a focus diameter of about 20 μm) could be adjusted to excite only an individual QD.

(ii) Second we have studied arrays of cylindrical QD's fabricated from shallow $In_{0.03}Ga_{0.97}As/GaAs$ QW's with a width of 5 nm. In these QW structures the half-width of the luminescence emission is small (about 1 meV), because X scattering by interface roughnesses or alloy fluctuations is considerably reduced in comparison to QW's with large In contents. When fabricating lateral nanostructures from these shallow wells, we find that the increase of the inhomogeneous broadening with decreasing structure size is weaker than in structures formed from deep wells. Therefore also spectrally closely spaced features can be resolved in spectra from arrays of shallow QD's. The size of the arrays was 25 $\times$25 μm. The diameter of the laser spot was chosen to be slightly larger than the array size in order to obtain homogeneous excitation conditions.

The geometric shape of the QD's determines the set of ''good'' quantum numbers, which describe the single-particle states in addition to the spin. Besides the vertical QW quantum number n_z the states are characterized by a radial and an azimuthal quantum number, n_r and n_φ, in cylindrical QD's. The quantum number n_φ originates from ro-

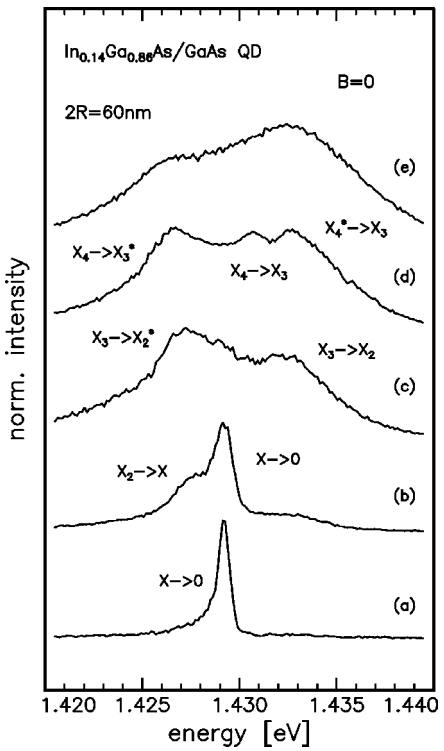

FIG. 1. PL spectra of a cylindrical $In_{0.14}Ga_{0.86}As/GaAs$ single QD with a diameter of 60 nm recorded at $B=0$ using varying excitation powers increasing from bottom to top: $P[\mu W]=10$ (a), 25 (b), 50 (c), 100 (d), and 200 (e).

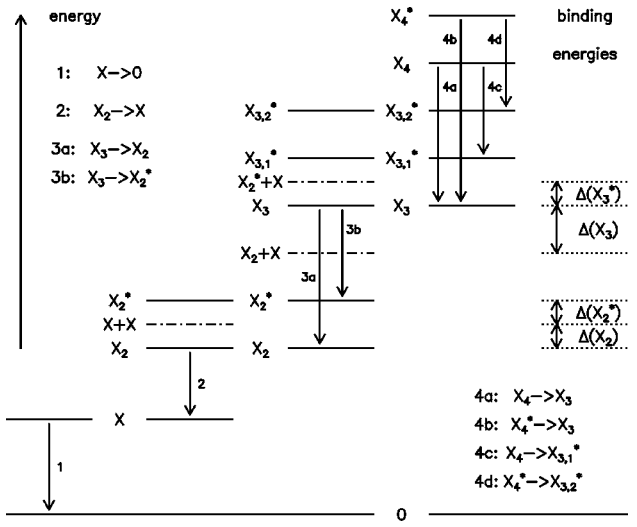

FIG. 2. Energy level scheme of QD multiX states $X_n^{(\star)}$ consisting of up to four X's at $B=0$. The first column corresponds to a carrier configuration, in which one e-h pair is in the QD, in the second and the third ones, respectively, two and three e-h pairs are in the dot and in the fourth column four e-h pairs populate the dot. The total energies of the states $E(X_n^{(\star)})$ are shown in vertical direction. The arrows indicate allowed optical transitions. The binding energies of the multiX states $\Delta(X_n^{(\star)})$ are shown on the right-hand side.

tation invariance around the QD symmetry axis normal to the QW plane. It corresponds to the angular momentum of the carriers around this axis. In rectangular QD's this symmetry is broken. The electronic levels are characterized by the quantum numbers n_x and n_y describing the excitations along the in-plane directions x and y.[30]

The lateral geometric sizes of the QD's were measured by scanning electron microscopy with an accuracy of ± 3 nm. The sizes ranged down to about 50 nm, slightly larger than the extension of the X wave function characterized by the Bohr radius of about 10–13 nm for the present $In_xGa_{1-x}As/GaAs$ structures.

III. TWO-EXCITON COMPLEXES

A. Biexciton binding energies at $B=0$

Figure 1 shows PL spectra of a cylindrical single QD with a diameter of 60 nm at $B=0$. At low excitation intensity (lowest trace in Fig. 1) a narrow emission line (labeled by $X\rightarrow 0$) is observed at an energy $E=1.429$ eV, which originates from recombination of one X in the QD. The half-width of the emission is about 0.6 meV.[31] With increasing excitation a second feature (labeled $X_2\rightarrow X$) appears on the low energy side of the X emission at $E=1.4275$ eV. The integrated intensity of this feature increases superlinearly with excitation power.[19] This dependence (together with the results of the studies in the magnetic field described below) clearly suggest that the emission can be attributed to biX recombination. In particular, it cannot be attributed to any excited X state in the QD because then it would appear on the high-energy side of the X line. We can also exclude X's bound to an impurity from consideration because the corresponding emission would appear even at the smallest excitation densities, which in our experiments is not the case.[32] Moreover, it cannot originate from charged X's[33] because if the QD would contain an equilibrium carrier (without photoexcitation) then the emission of charged X's would also appear already at the smallest illumination. For clarity, the spectra recorded at further elevated excitation intensities will be discussed in Sec. IV.

The low-energy shift of the emission $X_2\rightarrow X$ in comparison to the X emission arises from the X-X Coulomb interaction and can be considered as the biX binding energy $\Delta(X_2)$ in a QD,[34] as shown in Fig. 2. There the energies of the multiX states in cylindrical QD's are displayed schematically. From left to right the different columns correspond to carrier configurations in which one, two, three and four e-h pairs are in the dot. The allowed optical transitions due to the decay of an e-h pair are indicated by arrows. From the splitting between the X and the biX emission lines, we obtain the biX binding energy $\Delta(X_2)=2E(X)-E(X_2)=E(X\rightarrow 0)-E(X_2\rightarrow X)$, where $E(X_2)$ is the energy of the two-X complex and $E(X)$ is the X energy. For 60-nm-wide QD's we find a binding energy of about 1.6 meV.[35]

Figures 3–5 show PL spectra of different $In_{0.14}Ga_{0.86}As/GaAs$ single QD's of rectangular shape. The in-plane areas $A=L_xL_y$ of these dots were 45×55 nm^2 (Fig. 3), 50×70 nm^2 (Fig. 4) and 140×800 nm^2 (Fig. 5). The spectra were recorded at $B=0$ using different excitation intensities. Qualitatively, the behavior of the emission from the small dots is similar to that of cylindrical QD's. The low excitation PL spectra consist of the X emission line $X\rightarrow 0$ and with increasing excitation density the biX emission appears at the low-energy side of the X emission.

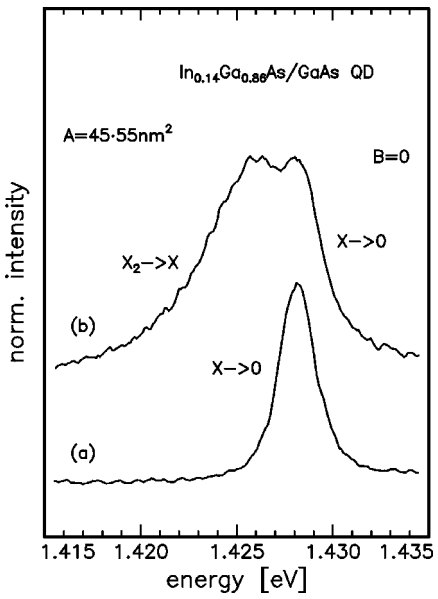

FIG. 3. PL spectra of a rectangular $In_{0.14}Ga_{0.86}As/GaAs$ single QD with an in-plane area of 45×55 nm^2 recorded at $B=0$ using varying excitation powers P increasing from bottom to top: $P[\mu W]=100$ (a), 400 (b).

Quantitatively, however, there are significant differences. Comparison of Figs. 3–5 shows that the energy gap between the biX and X emission lines depends strongly on the lateral dot size. In the smallest QD the $X_2\rightarrow X$ line lies about 2 meV below the X emission. In the larger dots the $X_2\rightarrow X$ line is

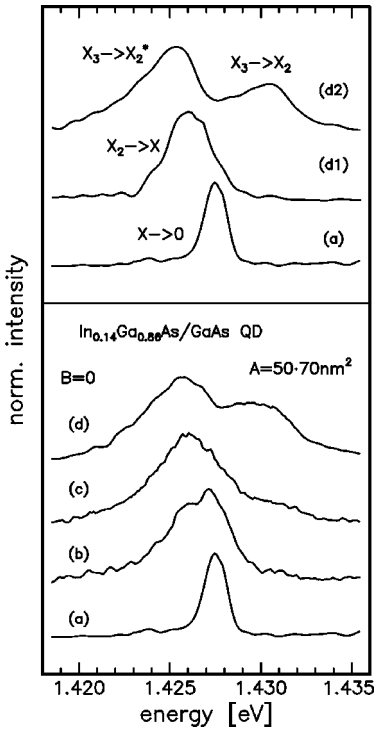

FIG. 4. PL spectra of a rectangular $In_{0.14}Ga_{0.86}As/GaAs$ single QD with an in-plane area of 50×70 nm^2 recorded at $B=0$ using varying excitation powers: $P[\mu W]=10$ (a), 25 (b), 50 (c), and 200 (d); the differential spectra d1 and d2 in the upper half of the figure are obtained from the spectra recorded at 25 μW and 50 μW excitation power.

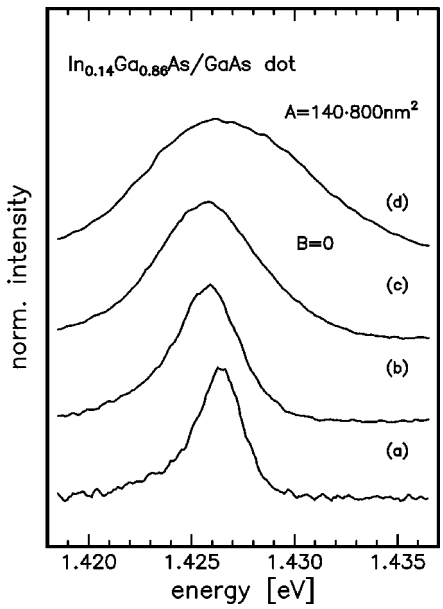

FIG. 5. PL spectra of a quasi-2D rectangular $In_{0.14}Ga_{0.86}As/GaAs$ single dot with an in-plane area of 140×800 nm^2 recorded at $B=0$ for varying excitation powers increasing from bottom to top: $P[\mu W]=10$ (a), 25 (b), 50 (c), and 200 (d).

located closer to the $X\rightarrow0$ line and is more difficult to resolve. In order to determine its energy with higher precision we have recorded differential spectra. In the upper half of Fig. 4 a typical differential spectrum ($d1$) is shown for a 50×70 nm^2 wide dot (difference of spectra recorded at P $=25$ μW and 10 μW). After subtracting the X emission, the biX line $X_2\rightarrow X$ dominates the spectrum. It is shifted by about 1.5 meV to lower energies in comparison to the X emission. In the large, quasi-2D dot the energy gap between $X_2\rightarrow X$ and $X\rightarrow0$ is about 0.7 meV.

The biX binding energies obtained from PL spectra of QD's are shown in Fig. 6 versus the lateral dot size. The squares give the results for rectangular QD's and the circles those for cylindrical QD's. In order to display the rectangular and the cylindrical dot data in one figure we calculate an effective diameter $2R$ for the rectangular QD's that describes the cross section of the structures $\pi R^2=L_xL_y$. Figure 6 shows that with decreasing lateral size the biX binding energy increases up to 2 meV for the smallest cylindrical QD's with a diameter of 50 nm. For a 2D $In_{0.10}Ga_{0.90}As/GaAs$ reference we find a binding energy of about 0.7 meV. That is, in these QD's $\Delta(X_2)$ is up to three times larger than in the quasi-2D reference and up to one order of magnitude larger than in bulk.

In previous studies[36] we have found that the effects of confinement on X's in $In_xGa_{1-x}As/GaAs$ QD's become important for sizes as large as 100 nm, which is about ten times the Bohr radius. Figure 6 shows that similar to the X binding energies $\Delta(X_2)$ is already enhanced for 100 nm wide dots.[37] Qualitatively, the observed increase compares well with that observed in previous investigations of QD's.[9,14,17,18,29]

$\Delta(X_2)$ is determined by the complicated balance of the interactions between the carriers forming the biX. BiX's in higher-dimensional structures are stable, because the finite extension of the four-particle wave function allows a carrier distribution, in which the attractive exceed the repulsive in-

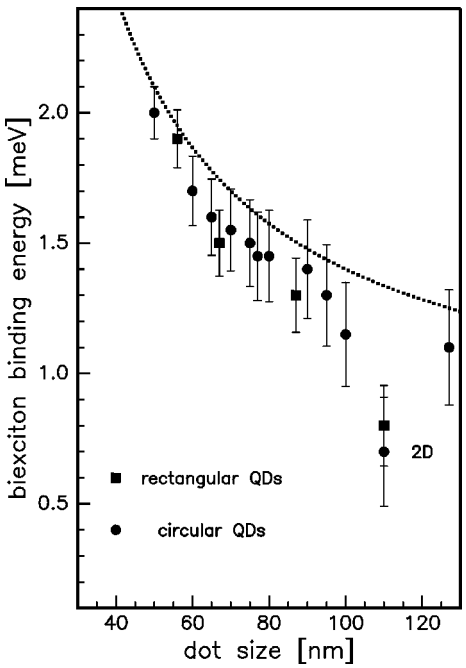

FIG. 6. BiX binding energies $\Delta(X_2)$ as function of the lateral dot size for cylindrical and rectangular $In_{0.14}Ga_{0.86}As/GaAs$ QD's. The dotted line gives the result of a theoretical estimate for $\Delta(X_2)$ described in the text.

teractions. By geometric confinement the interparticle distances are reduced and therefore the interparticle interactions are enhanced. In QW's this leads to a drastic enhancement of the biX binding energy over the bulk value.[5,6]

BiX's in QD's have been the subject of a number of theoretical investigations.[9–16] The biX binding energy has been determined using several calculation techniques, including matrix diagonalization, variational calculations, perturbation theory, and Monte Carlo techniques. All of these studies show that the QD biX also has a positive binding energy and that $\Delta(X_2)$ increases with decreasing dot radius R. The increase is to a good approximation proportional to $1/R$.

The dotted line in Fig. 6 gives the results of a fit to the data by a function proportional to $1/R$ with a binding energy of 0.7 meV for the 2D reference. From this fit good agreement with the experimental results is obtained. For the smallest QD's with a diameter of 50 nm (about four times the Bohr radius) the biX binding energy of 2 meV is about half the bulk Rydberg of 4 meV for $In_{0.14}Ga_{0.86}As$. This result is in agreement with the calculations of Takagahara[11] for spherical QD's with $R \sim 2a_X$.

The biX binding energy depends on the height of the confinement potential. Figure 7 shows PL spectra of an array of cylindrical $In_{0.03}Ga_{0.97}As/GaAs$ dots with a diameter $2R = 70$ nm. In these structures the QW confinement is rather weak. The evolution of emission lines with increasing illumination power is similar to that observed for single QD's. The narrow X emission $X \rightarrow 0$ dominates the spectrum at low excitation, and the biX emission $X_2 \rightarrow X$ appears at elevated excitation at the low-energy side of the X emission. Figure 8 shows high excitation spectra of $In_{0.03}Ga_{0.97}As/GaAs$ QD's with varying diameters at $B=0$. Due to the lateral quantization of the X the emission shifts to higher energies with

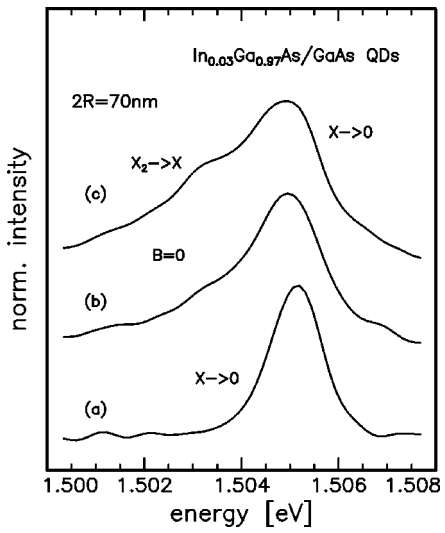

FIG. 7. PL spectra of an array of cylindrical $In_{0.03}Ga_{0.97}As/GaAs$ QD's with a diameter of 70 nm recorded at $B=0$ with varying excitation powers: $P[\mu W]=100$ (a), 200 (b), and 400 (c).

decreasing dot diameter, while the splitting between $X_2 \rightarrow X$ and $X \rightarrow 0$ does not vary strongly.

In Fig. 9 the dot size dependence of the biX binding energies is shown for $In_{0.03}Ga_{0.97}As/GaAs$ QD's. For comparison, also the data for $In_{0.14}Ga_{0.86}As/GaAs$ dots are plotted. The binding energies are shown in units of $\Delta(X_2)$ in the corresponding reference QW's. Within the experimental accuracy $\Delta(X_2)$ remains constant with decreasing size for the shallow dots. In strongly confined structures with lateral sizes larger than approximately the X Bohr radius both the attractive and the repulsive interactions increase. The redistribution of the biX wave function by the confinement leads to a net increase of $\Delta(X_2)$. In shallow $In_{0.03}Ga_{0.97}As/GaAs$ QW's the e wave function has a significant penetration into

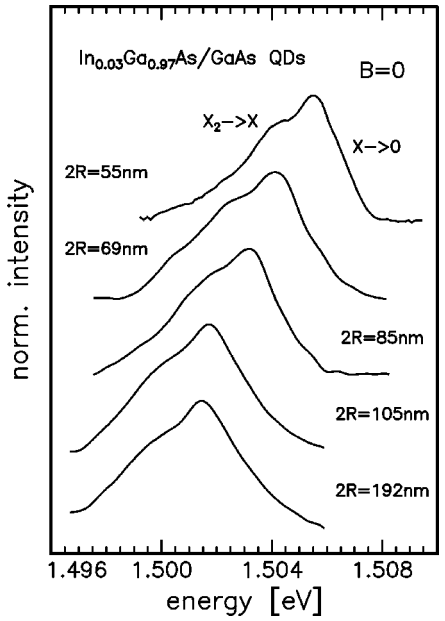

FIG. 8. High excitation PL spectra of cylindrical $In_{0.03}Ga_{0.97}As/GaAs$ QD's with varying diameters at $B=0$. The excitation power was 400 μW in each case.

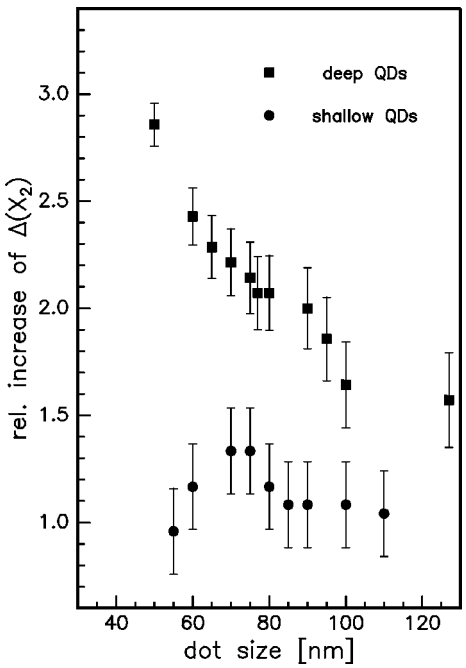

FIG. 9. BiX binding energies $\Delta(X_2)$ as functions of the lateral dot size for deep $In_{0.14}Ga_{0.86}As/GaAs$ and shallow $In_{0.03}Ga_{0.97}As/GaAs$ QD's of cylindrical shape. The binding energies are given in units of the binding energy in the respective quasi-2D reference samples.

the surrounding barriers, while the h wave function is still well confined. The resulting mismatch of the e and h wave functions might lead to a stronger increase of the repulsive interactions by the lateral confinement in comparison to the attractive ones. This might result in a compensation of the increase of $\Delta(X_2)$ due to wave-function redistribution and in an independence of $\Delta(X_2)$ on lateral dot size. However, detailed numerical calculations are required to understand this behavior fully.

B. Biexcitons in magnetic field

1. Unpolarized spectra

In previous experiments we have studied the X spin-splitting in $In_xGa_{1-x}As/GaAs$ QD's with $x=0.10$. From these studies we find that the spin splitting has a strong size dependence, but still is rather small, e.g., in comparison to the splitting between the size-quantized QD states.[38] In the present structures the biX binding energy $\Delta(X_2)$ exceeds the spin splitting $\Delta E_{\pm}$ and the biX is expected to be a stable state for all field strengths. Further the investigation of biX's in magnetic field should be possible from unpolarized PL spectra.

PL spectra of rectangular single dots are shown in Figs. 10–12. The spectra were recorded using the same excitation conditions as for those at $B=0$ (Figs. 3–5), but at $B=6$ T. However, the spectral features are different from those at zero magnetic field. Figure 10 shows that in a QD with an in-plane area of 45×55 nm^2 the splitting of the $X_2\rightarrow X$ and the $X\rightarrow 0$ emission lines is clearly reduced by B. This indicates a strong decrease of the biX binding energy.

In the larger, 50×70-nm^2-wide dot the X and the biX emission are very close to each other. To resolve their energy

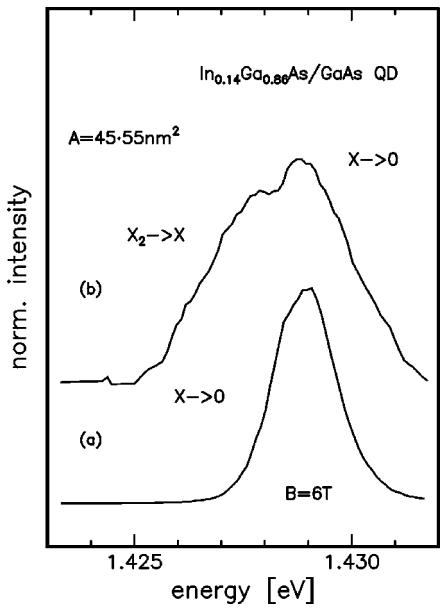

FIG. 10. PL spectra of a rectangular $In_{0.14}Ga_{0.86}As/GaAs$ single QD with an in-plane area of 45×55 nm^2 recorded at $B=6$ T with varying excitation powers: $P[\mu W]=100$ (a) and 400 (b).

splitting we have recorded a differential spectrum ($d1$). The biX is located at only slightly smaller energies (~ 0.6 meV) than the X emission. This splitting is significantly smaller than that (~ 1.5 meV) at $B=0$.

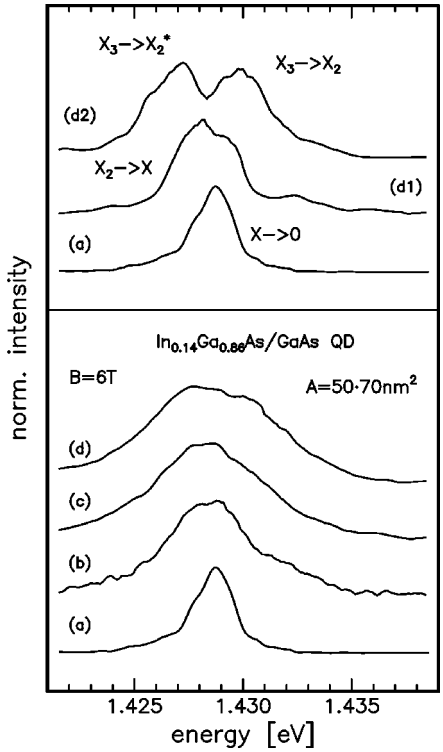

FIG. 11. PL spectra of a rectangular $In_{0.14}Ga_{0.86}As/GaAs$ single QD with an in-plane area of 50×70 nm^2 recorded at $B=6$ T with varying excitation powers: $P[\mu W]=10$ (a), 25 (b), 50 (c), and 200 (d); the differential spectra d1 and d2 in the upper half of the figure are obtained from the spectra recorded at 25 μW and 50 μW excitation power.

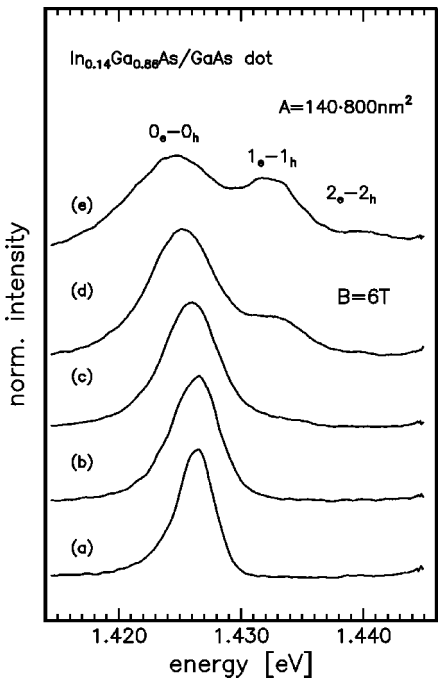

FIG. 12. PL spectra of a rectangular $In_{0.14}Ga_{0.86}As/GaAs$ single dot with an in-plane area of 140×800 nm^2 recorded at $B=6$ T for varying excitation powers increasing from bottom to top: $P[\mu W]=10$ (a), 25 (b), 50 (c), 100 (d), and 200 (e).

Two different effects could cause the reduction of the biX binding energy by B. First, a stronger diamagnetic shift of the biX in comparison to twice the shift of the X or second, the Zeeman-splitting of the emission lines could be the reason for the observed behavior. For clarification we have recorded polarized spectra of the X and biX emission.

2. Zeeman splitting of the biX emission

Figure 13 shows σ^+- and σ^--polarized PL spectra of $In_{0.03}Ga_{0.97}As/GaAs$ QD's at $B=8$ T for different excitation densities. At low excitation the spectra consist of the single

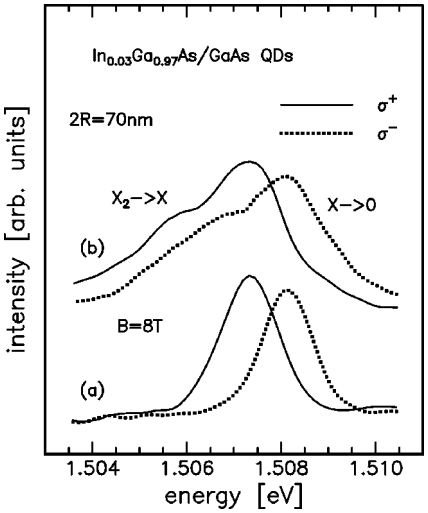

FIG. 13. Polarized PL spectra of an array of cylindrical $In_{0.03}Ga_{0.97}As/GaAs$ QD's with a diameter of 70 nm recorded at $B=8$ T using various excitation powers: $P[\mu W]=100$ (a) and 400 (b).

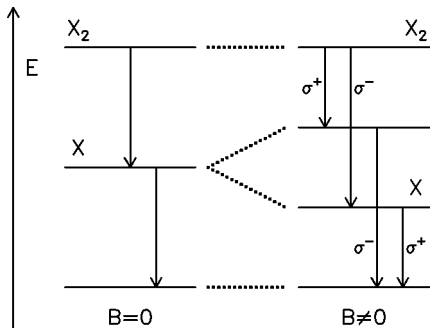

FIG. 14. Scheme of allowed optical transitions of X's and biX's in QD's at zero and nonzero magnetic fields. The total energies of the states are shown in vertical direction. Also the polarizations of the emission lines at $B\neq0$ are shown.

X emission line $[X\rightarrow0](\sigma^+)$ and $[X\rightarrow0](\sigma^-)$, respectively. The splitting $\Delta E_\pm$ of the lines arises from the Zeeman splitting of the X state $\Delta E_\pm=g_X\mu_B B$ where μ_B is the Bohr magneton and g_X is the X g factor. Within the experimental accuracy, the experimentally observed splitting $\Delta E_\pm$ increases linearly with magnetic field and is about 0.8 meV at $B=8$ T. The larger intensity of the σ^+ polarized component reflects a higher time-averaged filling of the X ground state. In spectra recorded at higher excitation intensities the σ^+- and σ^--polarized biX emission lines $[X_2\rightarrow X(\sigma^-)](\sigma^+)$ and $[X_2\rightarrow X(\sigma^+)](\sigma^-)$ are observed. The splitting of the biX emission lines is approximately equal to the splitting of the X emission, independent of the dot size.

This behavior can be understood from the scheme of optical transitions in Fig. 14. The biX ground state is a spin-singlet state and its energy cannot be split by B. However, the final state of the biX transition is an X, whose energy is split by B. Thus the splitting of the biX emission is given by that of the X in the final state of the optical transition. This interpretation is supported by Fig. 13, which shows that (in contrast to the X emission) the intensities of the spin-polarized biX emission lines are about equal as expected for transitions from the same initial state.

These results are therefore also an additional proof that the emission at the low-energy side of the X comes indeed from biX recombination. In particular, it should be noted that the emission cannot be associated with emission from trions consisting of an X and an e or a h. In that case the lines with σ^+ and σ^- polarizations would correspond to recombination of trions in the ground and excited spin states and therefore their intensities would be different.

Within this frame also the reduction of the biX binding energy by B has to be explained. The transition scheme in Fig. 14 shows that the $[X_2\rightarrow X(\sigma^+)](\sigma^-)$ emission line corresponds to a transition from the biX to an X in its spin ground state. The energy gap between the $[X_2\rightarrow X(\sigma^+)](\sigma^-)$ and $[X\rightarrow0](\sigma^+)$ emission lines can be considered as the effective biX binding energy, $\Delta(X_2)=E([X\rightarrow0](\sigma^+))-E([X_2\rightarrow X(\sigma^+)](\sigma^-))$ Further, the energy gap $\Delta^0(X_2)=E([X\rightarrow0](\sigma^\pm))-E([X_2\rightarrow X(\sigma^\mp)](\sigma^\pm))$ between the X and biX emission lines of the same polarization can be compared with $\Delta(X_2)$. $\Delta(X_2)$ and $\Delta^0(X_2)$ are shown in Fig. 15 versus magnetic field for 70-nm-wide $In_{0.03}Ga_{0.97}As/GaAs$ QD's. $\Delta(X_2)$ decreases about linearly from 1.3 meV to 0.5 meV up to 8 T. This decrease is equal

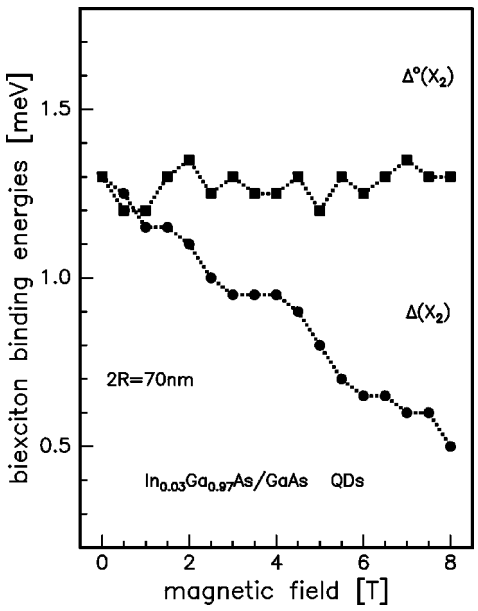

FIG. 15. BiX binding energy, $\Delta(X_2)$ and energy splitting $\Delta^0(X_2)$ as function of the magnetic field for 70 nm wide, cylindrical $In_{0.03}Ga_{0.97}As/GaAs$ QD's.

to the X spin splitting. In contrast, we find that $\Delta^0(X_2)$ is equal to $\Delta^0(X_2)$ at $B=0$. This result means that the decrease of the biX binding energy by a magnetic field originates mainly from the Zeeman splitting of the X, while the rearrangement of the biX and X wave functions by B plays a minor role and the resulting diamagnetic shifts of $E(X_2)$ and $2E(X)$ are equal.

This finding is confirmed by the magnetic-field dependence of $\Delta(X_2)$ in rectangular QD's as shown in Fig. 16. For all structures we find a decrease of $\Delta(X_2)$ with increasing B. However, the size of the decrease is strongly enhanced with decreasing dot size. For the quasi-2D dot we find a decrease

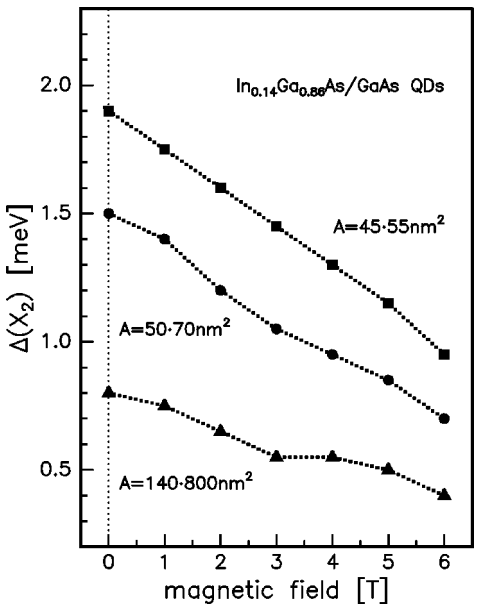

FIG. 16. BiX binding energies in rectangular $In_{0.14}Ga_{0.86}As/GaAs$ QD's with different in-plane areas as functions of the magnetic field.

from 0.8 meV at $B=0$ to 0.4 meV at $B=6$ T. For the dots with in-plane areas of 50×70 nm^2 and 45×55 nm^2 we find decreases of 0.8 meV and 1.2 meV, respectively. According to the above results this means that the X spin-splitting increases strongly with decreasing dot diameter. Such an increase has been observed in previous investigations of cylindrical $In_{0.10}Ga_{0.90}As/GaAs$ QD's,[38] in which an enhancement of the spin splitting over that in a QW was found that is inversely proportional to the square of the dot radius.

IV. MULTIEXCITONS IN QUANTUM DOTS

In the following the interaction energies of X's are investigated when the QD's are filled with more than two e-h pairs. In semiconductor structures with simple valence- and conduction-band structures and with free dispersion along at least one spatial direction (in bulk, in QW's and in quantum wires) the formation of such complexes is impossible because the strong Pauli repulsion among X's with the same spin orientation causes a separation of these X's in space.

A. Multiexcitons at zero magnetic field

When the excitation power is increased above the illumination densities at which biX emission is observed, additional emission lines appear in the QD luminescence spectra, as seen for a 60-nm-wide cylindrical QD in Fig. 1. A well-separated spectral line (labeled $X_3\rightarrow X_2$) appears at about $E=1.433$ eV, 3.5 meV above the X emission line $X\rightarrow0$. This emission cannot be attributed to the first excited state of the center-of-mass quantized motion of the X, because calculations show that for this dot diameter the energy separation of this state from the ground state would be less than 1 meV. In contrast, the separation of 3.5 meV is rather comparable to the sum of the quantized e and h single-particle energies. Simultaneously, the low-energy emission (labeled by $X_3\rightarrow X_2^\star$) is additionally redshifted by about 1 meV in comparison to the biX emission. The intensity of the low-energy feature saturates, when the excitation power is further increased, while that of the high-energy feature increases further.

These observations can only be explained by assuming that the e and h ground states in the QD (which are double spin degenerate) are fully occupied and additional carriers in the QD occupy the first excited states. The carriers in the ground and excited states form multiX complexes due to their mutual Coulomb interactions. In particular, the high-energy feature cannot be attributed to excited biexciton states, because then the appearance of this feature would not be accompanied by a further low-energy shift of the ground-state emission. The redshift of $X_3\rightarrow X_2^\star$ can only arise from Coulomb interactions with additional carriers in the dot.[39]

In cylindrical QD's the first excited states can be populated by up to four carriers due to spin and orbital angular momentum ($n_\varphi=\pm1$) degeneracies. From the comparison of the intensities of the excited state to the saturated ground-state emission, I_1 to I_0, one can estimate the (time-averaged) number of X's in the QD. In spectrum (c) I_1 is about half I_0 indicating that the excited state is filled with one e-h pair, while in spectrum (d) two X's are in the excited shell because of the equal intensities I_0 and I_1. At this excitation the

low-energy emission is again shifted to lower energies and the higher-lying emission line is split into two lines separated by almost 2 meV. A further increase of the excitation power causes a broadening of the spectral features. The ground-state emission cannot be resolved as a separate line anymore and the emission from excited states dominates. At the highest excitation the intensity I_1 is approximately twice as large as that of the ground-state emission indicating a strong filling of the first excited e and h shells. No fine structure can be resolved in the excited emission and its energy is about the energy of the emission $X_3 \rightarrow X_2$ of the three-exciton complex.

Similar observations are made for the three-X complex in rectangular QD's. Figure 4 shows that for a QD with an area of 50×70 nm^2 an increase of the excitation power results in the appearance of a well pronounced shoulder at the high-energy side of the X emission and in a shift of the ground-state emission to lower energies. In order to resolve both emission lines $X_3 \rightarrow X_2$ and $X_3 \rightarrow X_2^\star$ more clearly, we have again recorded a differential spectrum shown in Fig. 4, trace $d2$. The corresponding lines are located 2 meV below and 3 meV above the energy at which the $X \rightarrow 0$ transition is observed.

For comparison we have also performed high excitation studies of a large, quasi-2D rectangular dot. An increase of the excitation power causes changes of the optical spectra very similar to those in a QW. Figure 5 shows that no pronounced structure appears in the PL spectrum; the spectral line broadens monotonically and transforms into the structureless emission band characteristic of a Fermi system (e-h plasma) at $B=0$.[2]

B. Shell model for multiX states in QD's

For self-organized QD's with lateral sizes comparable to the X Bohr radius detailed calculations have shown that the X complexes have a shell structure that reflects the single particle density of states.[28] The splitting between the emission features from different shells corresponds to collective excitations of the exciton droplet in the QD. In first approximation the splitting is given by the energy difference between the single-particle states. Its renormalization by the Coulomb interaction is rather small. Thus the multiX states can be classified by using e and h single-particle rather than X shells. This shell model is therefore similar to that used earlier for multiX complexes bound at neutral impurities in bulk semiconductors.[40,41] Here we consider QD's in the weak-confinement regime with minimum lateral sizes of a few a_X. However, as discussed above the energy splitting between the excited and ground-state transitions is larger than the calculated energy splitting between the center-of-mass quantized X states, but instead is of the order of the sum of the quantized e and h energies. Thus our studies indicate that X complex formation on the basis of the single-particle shells occurs already for QD's with lateral sizes of a few Bohr radii. This may be expected from studies on bound multiX's in bulk semiconductors, where the Pauli repulsion among e's/h's prevents a strong spatial shrinkage of the wave function of the multiX complex.[40]

However, the energies of the multiX states are modified by the X-X Coulomb interaction. These interactions result in a renormalization of the transition energies and in a fine-structure splitting. For one or two e-h pairs the carriers occupy the lowest single-particle energy shells leading to the X and biX emission lines. As discussed above, the energy $E(X_2)$ of the biX state is smaller than the energy $2E(X)$ of two uncorrelated X's because of the attractive X-X interaction in the biX spin-singlet state.

With two carriers of opposite spin the e and h ground states ($n_z=0$, $n_r=0$, and $n_\varphi=0$ in cylindrical and $n_z=0$, $n_x=0$, and $n_y=0$ in rectangular QD's) are fully occupied. Therefore, when an additional e-h pair is created in the dot, the Pauli principle prevents the relaxation of these carriers into the ground, but forces them into the first excited states. The ground-state three-X complex X_3 thus consists of two e's and h's in the lowest and one e and h in the first excited shells $X_3 \equiv (2e,2h-1e^\star,1h^\star)$. Only transitions between carriers with the same quantum numbers have large oscillator strength and accordingly X_3 can decay in two different ways: First the recombination of an e and a h in the excited states can occur leaving the biX ground state X_2 as final state. This transition causes the high-energy feature $X_3 \rightarrow X_2$ in the spectra. Second, an e and a h in the ground shells can recombine leaving behind the excited biX state $X_2^\star \equiv (1e,1h-1e^\star,1h^\star)$ as a final state consisting of an e-h pair in both the ground and the first excited shells. The resulting spectral line, $X_3 \rightarrow X_2^\star$, has a smaller energy separation from the biX as the biX has from the X. This may be expected because the interaction energy between X's from inner and outer shells is weaker than the biX binding energy due to the reduced spatial overlap of the single-particle wave functions in the Coulomb interaction matrix elements.

From the transition energies we can determine the binding energies in the X complexes. From Fig. 2 the following relations are obtained: Besides the ground-state biX binding energy $\Delta(X_2)$ the biX binding energy $\Delta(X_2^\star)$ in the excited state can be calculated by $\Delta(X_2^\star)=E(X_3 \rightarrow X_2^\star)-E(X_3 \rightarrow X_2)+\Delta(X_2)$. The binding energy $\Delta(X_3)$ of a third X to the biX can be determined from $\Delta(X_3)=E(X \rightarrow 0)-E(X_3 \rightarrow X_2)$. Finally, we can consider the addition of a third e-h pair in the ground shells to the excited biX. Its binding energy $\Delta(X_3^\star)$ is given by $\Delta(X_3^\star)=E(X \rightarrow 0)-E(X_3 \rightarrow X_2^\star)$.

The dot size dependence of these binding energies in cylindrical $In_{0.14}Ga_{0.86}As/GaAs$ QD's is shown in Fig. 17. The X transition energies are determined from emission spectra at low excitation powers while the energies of the two- and three-X complexes are obtained from high excitation and from differential spectra.[35] While $\Delta(X_2)$ is positive (binding energy in a strict sense), the energy $\Delta(X_3)$ is negative (repulsion energy). This means that, similarly to the case of bulk, the effective X-X interaction in the QD is attractive only for biX's and the energy of the three-X state is larger than the energy of a biX and an X without correlation. The negative ''binding energy'' originates from the strong Pauli repulsion between e's/h's with identical spin orientation pushing the third X into a higher shell. The three-X complex is confined only because of the 3D geometric confinement potential, which prevents a spatial separation of X's. Similar arguments hold also for $\Delta(X_2^\star)$.

As expected from the biX binding energy, the correlation energies increase strongly with decreasing dot size because

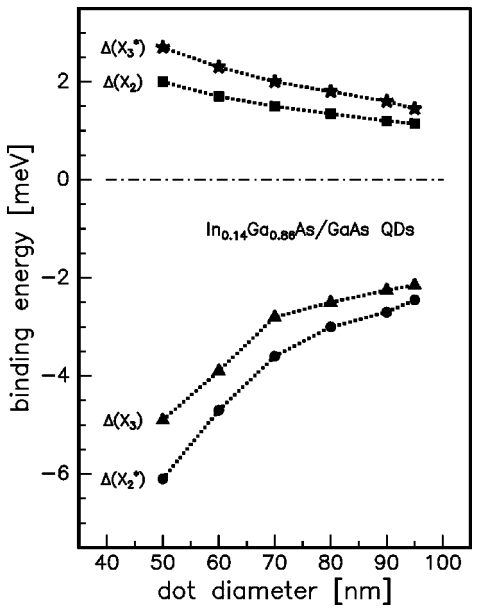

FIG. 17. Coulomb correlation energies $\Delta(X_n^{(\star)})$ of two- and three-X complexes as described in the text plotted against the diameter of cylindrical $In_{0.14}Ga_{0.86}As/GaAs$ QD's.

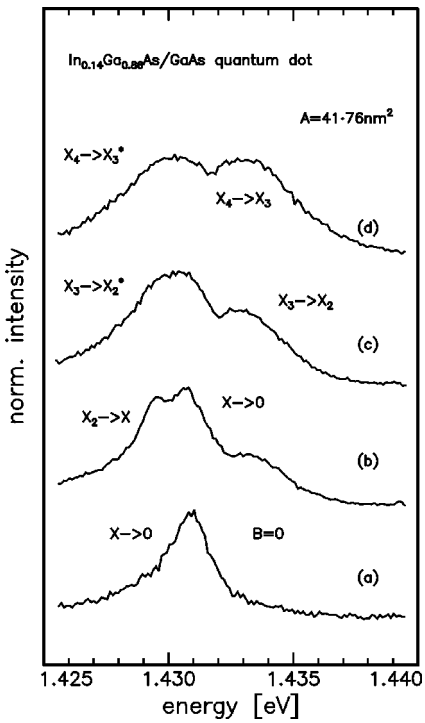

FIG. 18. PL spectra of a rectangular $In_{0.14}Ga_{0.86}As/GaAs$ single QD with an area of 41×76 nm^2 at zero magnetic field for varying excitation powers increasing from bottom to top: $P[\mu W]=25$ (a), 50 (b), 100 (c) and 200 (d).

of the spatial confinement. For example, $\Delta(X_3)$ increases from about -2 to -5 meV, $\Delta(X_2^\star)$ from -2.5 to more than -6 meV. According to the shell model the dominant contributions to $\Delta(X_3)$ and $\Delta(X_2^\star)$ are given by the energies of the quantized e and h single particle states, which increase with decreasing dot size as $1/r^2$.

The effective X interaction is attractive when an X is added in the ground shell to the excited biX. The third X fills an empty space and the Pauli repulsion has no effect whereas the correlation energy increases with the number of particles in the QD. Therefore $\Delta(X_3^\star)$ exceeds the biX binding energy by about 0.5 meV.

When even more e-h pairs populate the QD, additional carrier-carrier interactions must be taken into account. For a fourth e-h pair, the additional carriers also occupy the first excited single-particle states. In a cylindrical QD the first excited state is four times degenerate. Thus the additional e, for example, can occupy different states. First, it can occupy a state with a spin quantum number different from that of the third e (thus fulfilling the restrictions of the Pauli principle) but with the same orbital angular momentum. In this case the two e's in the excited shell can spatially come very close to each other leading to a strong repulsive e-e interaction which increases the energy of this state. Second, the fourth e can occupy a state with identical spin orientation but with different angular momentum. The Pauli repulsion then prevents the two excited e's coming close to each other and therefore the repulsive e-e interaction is smaller than in the first case. Therefore this carrier configuration is energetically preferable and forms the ground state four-X complex symbolically labeled $X_4\equiv(2e,2h-2e^\star\uparrow,2h^\star\uparrow)$, while the state with two excited e's of different spin orientations is an excited four-X complex $X_4^\star\equiv(2e,2h-e^\star\uparrow,e^\star\downarrow,h^\star\uparrow,h^\star\downarrow)$ with a higher energy.[42] The energy difference between these states corresponds to the exchange energy.

The radiative decay of four-X complexes can occur via recombination of an X from the inner or outer shell.[43] Optical transitions of outer shell X's leave a three-X complex in its ground state X_3 as final state and can occur with either X_4 or $X_4^\star$ being the initial state. Both transitions $X_4\rightarrow X_3$ and $X_4^\star\rightarrow X_3$ are observed in Fig. 1 and they are split due to the exchange energy splitting of the carriers in the four-X complex.[43] From the splitting of the lines the exchange energy is about 2 meV.

For optical transitions of X's from the inner shell the final state will be an excited three-X complex, either $X_{3,1}^\star\equiv(1e,1h-2e^\star\uparrow,2h^\star\uparrow)$ or $X_{3,2}^\star\equiv(1e,1h-e^\star\uparrow,e^\star\downarrow,h^\star\uparrow,h^\star\downarrow)$. The energy splitting between $X_{3,1}^\star$ and $X_{3,2}^\star$ is also determined by the exchange energy splitting and should be roughly equal to the splitting of X_4 and $X_4^\star$. Thus the allowed optical transitions $X_4\rightarrow X_{3,1}^\star$ and $X_4^\star\rightarrow X_{3,2}^\star$ have about the same energy and only one low-energy emission line is observed in the spectra. For this emission line a further small shift to lower energies is found compared to the emission line $X_3\rightarrow X_2^\star$. This redshift can be expected because the interaction between X's in the ground and excited shell is attractive.

For rectangular QD's with different side lengths the only degeneracy is the spin degeneracy, except for specific ratios of the lateral sizes for which degeneracies can occur. The first excited state is only twice degenerate and the spin of the fourth e in the dot must have an orientation opposite to that of the third e. Thus an exchange energy splitting of the four-X complex cannot occur in rectangular QD's. Typical PL spectra of a rectangular single QD with a cross section of 41×76 nm^2 are shown in Fig. 18. Qualitatively, the evolution of the dot emission is similar to that in cylindrical structures. First the X and biX features are observed in spectra (a) and (b). Then the excited shell states are populated leading to

the emission of three- and four-X complexes [spectra (b)–(d)]. As expected, the four-X complex emission consists only of two spectral lines, a low-energy feature $X_4 \rightarrow X_3^{\star}$ from the decay of an inner X and a high-energy feature $X_4 \rightarrow X_3$ from an outer X decay. For the latter transition no exchange energy splitting is found.

For the cylindrical QD's the first excited single particle shells can be occupied by two more carriers with increasing optical excitation. However, as can be seen for the 60-nm-wide $In_{0.14}Ga_{0.86}As/GaAs$ QD in Fig. 1, trace (e), then the spectral features broaden. The high excitation causes rather high carrier temperatures, which lead to a population also of higher excited states. The resulting large number of possible transitions might result in the observed broadening. The emission from the ground shell can no longer be resolved as a separate line. The energy of the excited shell transition is about the energy of the excited shell transition of the three-exciton-complex and no fine structure is resolved in the emission line. As discussed above, the ratio of emission intensities I_1 to I_0 indicates a strong filling of the first excited state. According to the shell model for dots in the strong-confinement regime, the energy of the emission from a shell filled with one X is the same as that of emission from a completely filled shell, for which the final state is a shell with one vacancy.[28] This is a direct consequence of the hidden symmetries of the multiparticle Hamiltonian. Indications for this behavior can also be found for the present QD's in the weak-confinement regime. However, further studies are necessary to verify this feature clearly in the optical spectra.

When the lateral dot size becomes much larger than the X Bohr radius, the influence of the geometric confinement potential on the single particle states can be neglected. The energy spectrum is quasicontinuous and the dots can be occupied with a large number of X's of the same spin orientation that are spatially separated. With increasing excitation the carrier configuration in large dots transforms from a system of X's over a system of biX's into an e-h plasma, as observed experimentally in Fig. 5.

C. Magnetic-field dependence of multiexciton energies

A test for the above shell model is the magnetic-field dependence of the multiX energies. A magnetic field can lift degeneracies of QD levels leading the electronic system back to a ''quasicontinuous'' single-particle energy spectrum.[21,25,44–46] The hidden symmetries in the multiparticle Hamiltonian are destroyed for QD's in the strong-confinement regime, except for certain magnetic fields, at which degeneracies of electronic states occur.[28] In the limit of a very stong magnetic field the symmetry is fully broken. The excitons then form a maximum density droplet. Thus a magnetic field results in a significant modification of the multiX shells.

The evolution of the three-X-complex energies with increasing B can be seen from the PL spectra of a rectangular dot with an area of 50×70 nm^2. Comparison of the differential spectra $d2$ in Figs. 4 and 9 shows that the energy splitting of the emission lines $X_3 \rightarrow X_2^{\star}$ and $X_3 \rightarrow X_2$ is significantly reduced at $B=6$ T in comparison to $B=0$. This decrease means that the magnetic field suppresses the repulsion between X's with the same spin orientation.

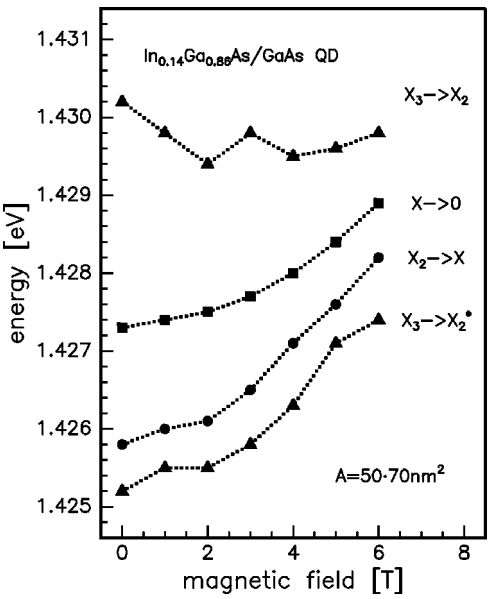

FIG. 19. Transition energies of the spectral lines due to decay of two- or three-X complexes in a rectangular $In_{0.14}Ga_{0.86}As/GaAs$ single QD with an area of 50×70 nm^2 as functions of the magnetic field.

The transition energies of the X complexes in a rectangular QD with an area of 50×70 nm^2 are shown in Fig. 19 versus B. The $X \rightarrow 0$ and $X_2 \rightarrow X$ transitions shift smoothly to higher energies with increasing B. For the transition of the three-X complex into the excited biX complex $X_3 \rightarrow X_2^{\star}$ also a small shift to higher energies is observed, which is similar to that of $X_2 \rightarrow X$. In contrast, the energy of the $X_3 \rightarrow X_2$ transition decreases at low B and shifts to higher energies only at high fields.

In the frame of the shell model the magnetic-field dependence of the energy splitting between multiX emission lines is mainly given by that of the single-particle energies. A magnetic field causes the convergence of QD states to form Landau levels (LL's) when the magnetic length $\ell_B = (\hbar/eB)^{1/2}$ becomes smaller than the QD size. The energy splitting between the first excited and the ground e and h states, $\Delta E = \Delta E_e + \Delta E_h$, decreases continuously with increasing B. For example, in cylindrical QD's the degeneracy of states with positive and negative angular momenta n_{φ} is lifted by the magnetic-field interaction of the magnetic moment associated to n_{φ}. The first excited state with $n_{\varphi}=-1$ converges with the ground state $n_{\varphi}=0$ to form the lowest LL.[44,21] In contrast, the state with $n_{\varphi}=+1$ transforms into the first excited LL.

From the transition energies in Fig. 19 the magnetic-field dependence of the Coulomb correlation energies can be derived. All binding/repulsion energies, shown in Fig. 20, tend to zero with increasing B. For the repulsion energy $\Delta(X_3)$ in the three-X complex we find a decrease from -3 meV to -1 meV. For the binding energy of the excited biX state $\Delta(X_2^{*})$ we find a similar decrease by about 2 meV. By a magnetic field the particles are localized in an area with an extension of about $2\ell_B$. The Pauli repulsion is reduced when ℓ_B becomes smaller than the QD size and the behavior of the carriers becomes more and more QW-like. Consequently $\Delta(X_3)$ and also $\Delta(X_2^{\star})$ decrease with B and tend to

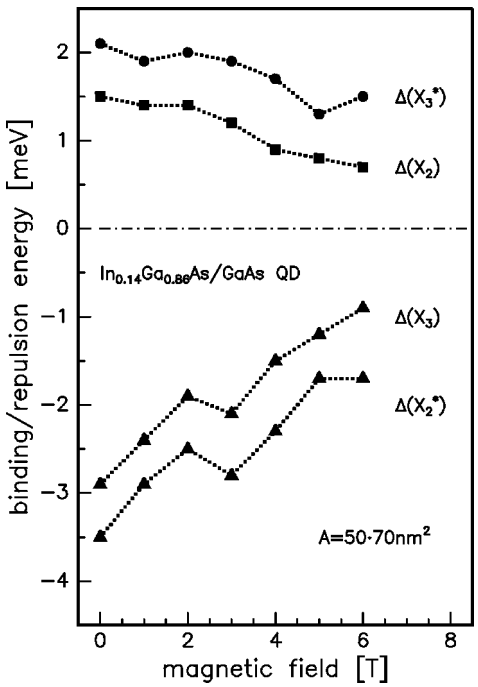

FIG. 20. Coulomb correlation energies $\Delta(X_n^{(\star)})$ of two- and three-X complexes in an $In_{0.14}Ga_{0.86}As/GaAs$ rectangular single QD with an area of 50×70 nm^2 vs magnetic field.

zero for $L,R\gg\ell_B$, that is, when the X's in the QD are separated by several magnetic lengths. A similar transitionlike behavior with increasing B has recently been found for X's in quantum wires.[47]

Finally the B dependence of $\Delta(X_3^{\star})$, the binding energy of an X in the ground state to an excited biX, can be considered. $\Delta(X_3^{\star})$ is slightly more than 2 meV at $B=0$ and is reduced to about 1.5 meV at $B=6$ T. It follows closely the magnetic-field dependence of $\Delta(X_2)$. As for the biX, $\Delta(X_3^{\star})$ is reduced by the X Zeeman splitting, while the additional attractive interaction with the X in the excited shell is not strongly modified by B.

For comparison also a large, quasi-2D dot has been studied in high magnetic fields. For this QD the PL spectra in Fig. 10 are qualitatively different from that of small QD's, but are similar to those of a QW.[48] In particular, in high excitation spectra a spectral line appears only at much higher energies than in a small dot. The energy of this spectral line increases linearly with B and the energy splitting from the ground-state transition is comparable to the sum of the e and h cyclotron energies, $\hbar\omega_c=\hbar eB/\mu$, where μ is the reduced e and h mass. Hence the spectral features can be assigned to emission from the ground, first, and second excited LL's. The emission lines are labeled accordingly, $n_e-n_h,n_i=0,1,2$, corresponding to the e and h LL quantum numbers. From the filling of the LL's at the highest excitation we estimate that the dot is occupied by a few hundred e-h pairs.[49]

The broadening of the lowest LL emission line is relatively small until carriers occupy the first Landau level and form a maximum density droplet.[50–53] This means that the effective X-X interaction in the lowest LL is strongly suppressed. Only when the first excited LL is occupied with carriers a significant low-energy shift of the ground-state transition in conjunction with a strong broadening of the emission line is observed that arises from the interaction of particles in different LL's. This behavior occurs because the e-e and h-h interactions cancel exactly the e-h interactions among X's in one LL and the X's form an ideal gas.

V. CONCLUSIONS

MultiX complexes in $In_xGa_{1-x}As/GaAs$ QD's with lateral dimensions down to 50 nm have been investigated by PL spectroscopy. A model is discussed that explains the experimental findings by an X complex formation on the basis of e and h single-particle shells. The formation of biX's at $B=0$ has been observed with binding energies that increase with decreasing dot size. The biX binding energies are decreased by a magnetic field normal to the QD plane. This decrease originates mainly from the Zeeman splitting of the X emission. MultiX complexes are confined in QD's only because of the 3D geometric confinement potential. Their binding energies are negative because the Pauli repulsion pushes additional e's and h's into higher shells. The Coulomb correlation energies among the carriers forming the complexes increase with decreasing dot size. A magnetic field reduces strongly the X-X repulsion in the multiX complexes when the magnetic length becomes smaller than the QD size.

ACKNOWLEDGMENTS

The work was supported by the State of Bavaria and partly by the Volkswagen Foundation and NATO.

[1] For an overview see, for example, *23rd International Conference on the Physics of Semiconductors*, edited by M. Scheffler and R. Zimmermann (World Scientific, Singapore, 1996), Vol. 2, Chap. IV.

[2] See, for example, C.F. Klingshirn, *Semiconductor Optics* (Springer-Verlag, Berlin, 1995).

[3] P. A. Maksym and T. Chakraborty, Phys. Rev. Lett. **65**, 108 (1990).

[4] P. Hawrylak and D. Pfannkuche, Phys. Rev. Lett. **70**, 485 (1993).

[5] R. C. Miller, D. A. Kleinman, A. C. Gossard, and O. Munteanu, Phys. Rev. B **25**, 6545 (1982).

[6] D. Birkedal, J. Singh, V. G. Lyssenko, J. Erland, and J. M. Hvam, Phys. Rev. Lett. **76**, 672 (1996), and references therein.

[7] L. Banyai, I. Galbraith, C. Ell, and H. Haug, Phys. Rev. B **36**, 6099 (1987).

[8] F. L. Madarasz, F. Szmulowicz, and F. K. Hopkins, Phys. Rev. B **52**, 8964 (1995).

[9] U. Woggon, in *Optical Properties of Semiconductor Quantum Dots*, Springer Tracts in Modern Physics (Springer-Verlag, Berlin, 1997), Vol. 136.

[10] L. Bányai, Y. Z. Hu, M. Lindberg, and S. W. Koch, Phys. Rev. B **38**, 8142 (1988); L. Banyai, *ibid.* **39**, 8022 (1989).

[11] T. Takagahara, Phys. Rev. B **39**, 10 206 (1989).
[12] Al. L. Efros and A. V. Rodina, Solid State Commun. **72**, 645 (1989).
[13] G. W. Bryant, Phys. Rev. B **41**, 1243 (1990).
[14] Y. Z. Hu, S. W. Koch, M. Lindberg, N. Peyghambarian, E. L. Pollock, and F. Abraham, Phys. Rev. Lett. **64**, 1805 (1990). Y. Z. Hu, M. Lindberg, and S. W. Koch, Phys. Rev. B **42**, 1713 (1990).
[15] E. L. Pollock and S. W. Koch, J. Chem. Phys. **94**, 6776 (1991).
[16] S. V. Nair and T. Takagahara, Phys. Rev. B **53**, 10 516 (1996); **55**, 5153 (1997).
[17] Y. Masumoto, S. Okamoto, and S. Katayanagi, Phys. Rev. B **50**, 18 658 (1994); Y. Masumoto, T. Kawamura, and K. Era, Appl. Phys. Lett. **62**, 225 (1993).
[18] K. Brunner, G. Abstreiter, G. Böhm, G. Tränkle, and G. Weimann, Phys. Rev. Lett. **73**, 1138 (1994).
[19] R. Steffen, A. Forchel, T. L. Reinecke, T. Koch, M. Albrecht, J. Oshinowo, and F. Faller, Phys. Rev. B **54**, 1510 (1996).
[20] U. Bockelmann, Ph. Roussignol, A. Filoramo, W. Heller, G. Abstreiter, K. Brunner, G. Böhm, and G. Weimann, Phys. Rev. Lett. **76**, 3622 (1996).
[21] M. Bayer, A. Schmidt, A. Forchel, F. Faller, T. L. Reinecke, P. A. Knipp, A. A. Dremin, and V. D. Kulakovskii, Phys. Rev. Lett. **74**, 3439 (1995).
[22] H. Lipsanen, M. Sopanen, and J. Ahopelto, Phys. Rev. B **51**, 13 868 (1995).
[23] S. Fafard, R. Leon, D. Leonard, J. L. Merz, and P. M. Petroff, Phys. Rev. B **52**, 5752 (1995).
[24] S. Raymond, S. Fafard, P. J. Poole, A. Wojs, P. Hawrylak, S. Charbonneau, D. Leonard, R. Leon, P. M. Petroff, and J. L. Merz, Phys. Rev. B **54**, 11 548 (1996).
[25] R. Rinaldi, P. V. Giugno, R. Cingolani, H. Lipsanen, M. Sopanen, J. Tulkki, and J. Ahopelto, Phys. Rev. Lett. **77**, 342 (1996).
[26] M. Ikezawa, Y. Masumoto, T. Takagahara, and S. Nair, Phys. Rev. Lett. **79**, 3522 (1997).
[27] A. Barenco and M. A. Dupertuis, Phys. Rev. B **52**, 2766 (1995).
[28] A. Wojs and P. Hawrylak, Solid State Electron. **100**, 487 (1996); S. Raymond, P. Hawrylak, C. Gould, S. Fafard, A. Sachrajda, M. Potemski, A. Wojs, S. Charbonneau, D. Leonard, P. M. Petroff, and J. L. Merz, Solid State Commun. **101**, 883 (1996).
[29] R. Steffen, T. Koch, J. Oshinowo, and A. Forchel, Appl. Phys. Lett. **68**, 223 (1996).
[30] Note that the usage of quantum numbers (n_r, n_φ, n_z) and (n_x, n_y, n_z) is only adaquate for QD's having a strong confinement potential. For such structures Schrödinger's equation is separable. This does not hold for shallow QD's, for which the motions along different directions are coupled and the above quantum numbers can be used only approximately.
[31] The full widths at half-maximum of the QD emission at low excitation range from 0.5–2.5 meV. These linewidths are significantly reduced in comparison to those observed earlier in studies of arrays of etched QD's (Ref. 21). However, they are still larger than, for example, the linewidths in natural QD's (Ref. 54). The larger linewidth may originate from fluctuations of the QD potential in time, which arise from photoexcited surface charges.
[32] Note that for certain single QD's a different behavior of the emission spectrum was found with increasing excitation power: A spectral line on the low-energy side of the X emission is observed that dominates at low excitations. This feature may originate from an impurity in the QD. The energy of a photoexcited X in the QD is reduced due to interaction with this impurity. The energy of a second e-h pair in the QD is larger than that of the first e-h pair.
[33] In a quasi-2D system a density of free e's or h's is required for the formation of charged X's (Ref. 55), which can be excluded for the present undoped QW structures, from which the QD structures were fabricated. Thus an assignment of the low-energy feature to trionic emission can be excluded. Charged X's in QD's have been studied both experimentally and theoretically (Refs. 56–59).
[34] Due to the 3D confinement the separation between e's and h's in the QD cannot be increased to infinity. Therefore the X binding energy cannot be defined as the energy difference between the onset of continuum of states and the lowest X state, but rather can be understood as energy difference between a noninteracting e-h pair and an e-h pair interacting by the Coulomb attraction. In this sense also a biX or multiX binding energy can be defined.
[35] The energies of the emission lines have been determined directly from each spectrum and have been checked by detailed lineshape analysis.
[36] M. Bayer, S. N. Walck, T. L. Reinecke, and A. Forchel, Phys. Rev. B **57**, 6584 (1998).
[37] For the cylindrical and rectangular InGaAs quantum disks studied here the optically active region is sandwiched between GaAs layers. The height of the $In_xGa_{1-x}As$ layer is at least one order of magnitude smaller than the lateral box sizes. In previous studies (Ref. 36) we found that the effects of image charges at the lateral sidewalls that appear due to the large discontinuity of the dielectric function there are negligible.
[38] M. Bayer, V. B. Timofeev, T. Gutbrod, A. Forchel, R. Steffen, and J. Oshinowo, Phys. Rev. B **52**, 11 623 (1995).
[39] In addition, for an excited biX complex the low-energy emission would shift to higher energies in comparison to the biX emission, because the X-X interaction is weaker for X's from different shells than from the same shells.
[40] For an overview see, for example, D. C. Reynolds, C. W. Litton, R. J. Almassy, S. B. Nam, P. J. Dean, and R. C. Clarke, Phys. Rev. B **13**, 2507 (1976); H. P. Gislason, B. Monemar, M. E. Pistol, A. Kana'ah, and B. C. Cavenett, *ibid.* **33**, 1233 (1986); J. Gutowski, N. Presser, and I. Broser, *ibid.* **38**, 9746 (1988); J. A. Wolk, T. W. Steiner, and M. L. W. Thewalt, *ibid.* **50**, 18 030 (1994).
[41] For an overview of multiexciton complexes in indirect semiconductors see, for example, M. L. W. Thewalt, Phys. Rev. Lett. **38**, 521 (1977); M. L. W. Thewalt and J. A. Rostoworoski, *ibid.* **41**, 808 (1978); V. D. Kulakovskii, G. E. Pikus, and V. B. Timofeev, Usp. Fiz. Nauk. **135**, 237 (1981) [Sov. Phys. Usp. **24**, 815 (1981)]; Y.-C. Chang and T. C. Mc Gill, Phys. Rev. B **25**, 3963 (1982); Phys. Rev. Lett. **45**, 471 (1980); R. S. Pfeiffer and H. B. Shore, Phys. Rev. B **25**, 3897 (1982); V. A. Karasyuk and E. C. Lightowlers, *ibid.* **45**, 3319 (1992).
[42] This result is an analogon of the well-known Hund's rules for many-electron atoms. These rules give the energy order of all possible states formed by a certain number of e's in an atomic shell. The first rule states that among all e configurations the one with maximum spin has the lowest energy, in agreement with our result. The second rule states that among the states with identical spins the state with the highest angular momentum has the lowest energy.
[43] Apparently the carrier spins are not completely relaxed, because the four-exciton-complex emission lines $X_4 \rightarrow X_3$ and $X_4^\star \rightarrow X_3$

have about the same intensity and the carriers are not distributed thermically in the shells. This might be attributed to the rather high optical excitation necessary in order to populate the QD's with four e-h pairs. The high excitation might cause carrier temperatures, at which states with a splitting of about the exchange energy of 2 meV are almost equally populated. However, these temperatures cannot cause a dissociation of the multiX complexes because the carriers forming the complexes are three-dimensionally confined in the QD's.

[44] T. Demel, D. Heitmann, P. Grambow, and K. Ploog, Phys. Rev. Lett. **64**, 788 (1990).

[45] V. Halonen, T. Chakraborty, and P. Pietilainen, Phys. Rev. B **45**, 5980 (1992).

[46] U. Bockelmann, Phys. Rev. B **50**, 17 271 (1994).

[47] M. Bayer, Ch. Schlier, Ch. Gréus, A. Forchel, S. Benner, and H. Haug, Phys. Rev. B **55**, 13 180 (1997).

[48] See, for example, L. V. Butov, V. D. Kulakovskii, G. E. W. Bauer, A. Forchel, and D. Grutzmacher, Phys. Rev. B **46**, 12 765 (1992).

[49] Assuming spin degeneracy the number of carriers in a LL is given by $g = 4.838 \times 10^{10} B(1/\mathrm{cm}^2\ T)$. From this degeneracy we can estimate the number of carriers in the dot by multiplying g with the number of filled LL's (which is about 2 at the highest illumination) and the in-plane dot area. From this estimate we obtain a number of about 500 e-h pairs in the dot.

[50] I. V. Lerner and Yu. E. Lozovik, Zh. Éksp. Teor. Fiz. **80**, 1488 (1981) [Sov. Phys. JETP **53**, 763 (1981)].

[51] D. Paquet, T. M. Rice, and K. Ueda, Phys. Rev. B **32**, 5208 (1985).

[52] A. H. MacDonald and E. H. Rezayi, Phys. Rev. B **42**, 3224 (1990).

[53] Yu. A. Bychkov and E. I. Rashba, Phys. Rev. B **44**, 6212 (1991).

[54] A. Zrenner, L. V. Butov, M. Hagn, G. Abstreiter, G. Böhm, and G. Weimann, Phys. Rev. Lett. **72**, 3382 (1994).

[55] K. Kheng, R. T. Cox, Y. Merle d'Aubigné, F. Bassani, K. Saminadayar, and S. Tatarenko, Phys. Rev. Lett. **71**, 1752 (1993); G. Finkelstein, H. Shtrikman, and I. Bar-Joseph, *ibid.* **74**, 976 (1995); H. Buhmann, L. Mansouri, J. Wang, P. H. Beton, N. Mori, L. Eaves, M. Henini, and M. Potemski, Phys. Rev. B **51**, 7969 (1995).

[56] T. Kawazoe and Y. Masumoto, Phys. Rev. Lett. **77**, 4942 (1996).

[57] R. J. Warburton, C. S. Dürr, K. Karrai, J. P. Kotthaus, G. Medeiros-Ribeiro, and P. Petroff, Phys. Rev. Lett. **79**, 5282 (1997).

[58] A. Wojs and P. Hawrylak, Phys. Rev. B **51**, 10 880 (1995).

[59] Ph. Lelong and G. Bastard, Solid State Commun. **98**, 819 (1996).